

# Comparison of the Characteristics of FCAW and SAW for the Brittle Crack Propagation of Welded Parts of BCA Steel in Container Ships

Kyung-Shin Choi\*, Sang-Hoon Lee\*\*, JeongJu Choi\*\*\*,#

\*Changwon National University, \*\*Lloyd's Register, \*\*\*Dong-a University

## 컨테이너선의 후 물재 용접부 취성 균열 전파에 대한 FCAW와 SAW의 비교 특성에 관한 연구

최경신\*, 이상훈\*\*, 최정주\*\*\*,#

\*창원대학교, \*\*로이드 선급, \*\*\*동아대학교

(Received 25 November 2020; received in revised form 30 December 2020; accepted 06 January 2021)

### ABSTRACT

The size of container ships is increasing to increase the cargo loading capacity. However, container ships are limited in terms of the hull longitudinal strength. To overcome this limitation, brittle crack arrest steel can be used. This study was aimed at examining the influence of the heat input on the welding procedures of flux cored arc welding and submerged arc welding. In the experiment, the crack tip opening displacement test, which pertains to a parameter of fracture mechanics, was performed, and a 3-point bending tester was adopted. Based on the results, the crack measurement method was presented, and the stress expansion coefficient value for the pre-fatigue crack length was derived according to the heat input after the pre-cracking length was measured. It was noted that the heat input affected the crack tip opening displacement of brittle crack arrest steel.

**Key Words** : CTOD(균열 선단 열림 변위), Clip Gauge(변위 게이지), Brittle Crack Arrest(취성 균열 정지 인성), Flux Cored Arc Welding(플럭스 코어드 아크 용접), Fatigue(피로)

### 1. Introduction

Container ships are long in the bow and stern directions and have a highly vulnerable longitudinal strength due to their upper decks, which are open

for container loading. To compensate for this weakness, a thick plate and an extra thick plate of at least 50 mm and 100 mm, respectively, are used to satisfy the requirements of the insufficient longitudinal components. With the recent increase in container ship sizes, the thickness of the longitudinal components has continued to increase proportionally. For extra thick plates, the evaluation method of the

# Corresponding Author : jchoi72@dau.ac.kr

Tel: +82-51-200-7652, Fax: +82-52-200-6598

brittle crack arrest (BCA) weld structures is mainly a large-scale destruction test; however, some studies have shown difficulties in the brittle crack arrest of welds greater than 65 mm.<sup>[1-2]</sup> Other studies have demonstrated that if the brittle cracks along the weld joint extend, the cracks tend to penetrate the test plate at stress levels higher than 200 MPa, even if longitudinal components are present.<sup>[3]</sup> In the interest of improving the safety of the unstable fracture, the international association of classification societies established rules on the use of steel with brittle crack arrests of at least 460 MPa (yield strength) for a container ship. Additionally, a crack tip opening displacement (CTOD) test is required to ensure stability for the brittle crack arrest of high-tension steel. A CTOD is a higher impact-induced or breakage-induced experiment at temperatures lower than that of conventional steel.<sup>[4]</sup> While welding processes that can reduce the brittle crack arrest in the upper deck structure of container ships using crack arrest steel plates are being developed, the results of the CTOD studies on electro gas welding (EGW) have been verified.<sup>[5]</sup> there are also verified CTOD studies on flux cored arc welding (FCAW) and submerged arc welding (SAW).<sup>[6]</sup> In this study, we compared the characteristics of brittle fracture for welding processes (FCAW and SAW) in welds of high strength thick plates (YP40 BCA) that are suitable for the upper structure of container ships. Furthermore, CTOD experiments have been conducted to study the overall strength of irregularity between the weld metals in the heat-affected area.

## 2. Experimental methods

### 2.1 Properties of specimens

The specimens produced in this experiment used  
 $C_{eq} = C + Mn/6 + (Ni + Cu)/15 + (Cr + Mo + V)/5$   
 $P_{cm}(\%) = C + Si/30 + Mn/20 + Cu/20 + Ni/60 + Cr/20 + Mo/15 + V/10 + 5B$

**Table 3 Summary of the welding parameters**

Welding Process	Current (A)	Voltage (V)	Travel Speed (cm/min)
FCAW	290	33	48
SAW	880	33	50

EH40BCA-TMCP steel with a thickness of 80 mm applied to the container ship superstructure, with mechanical properties shown in Table 1 and chemical properties in Table 2.

### 2.2 Welding method

The welding groove configuration of the test plates used in this experiment is shown in Figure 1. For SAW, up to 2 passes were filled with FCAW to perform automatic welding. Generally, the heat input is 15 to 30 kJ; FCAW is up to 34.4 kJ/cm and SAW to 49.8 kJ/cm. The first pass of FCAW has a maximum heat input of 55.0 kJ/cm, as the steel is thick and heat-treated. In addition, the preheating and maximum interlayer temperatures are 127°C/170°C and 130°C/220°C for FCAW and SAW, respectively, with a groove angle of 30°, root face of 0~3mm, and root gap of 3~8mm. Detailed welding conditions are shown in Table 3.

### 2.3 Crack detection

In accordance with British Standard (BS) 7448 Part 1:1991, the pre-crack was derived from

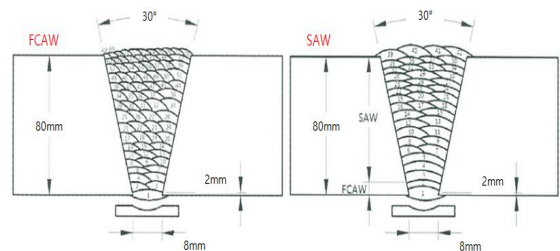


**Fig. 1 Details of weld joint FCAW and SAW**

the actual value of the test plate. The actual crack length Equation (1), taking the fatigue crack length to be length ( $a_o$ , mm) was obtained by summing the machining notch length (mm) and fatigue crack length (mm), as shown in Equation (2).

$$a_f = \frac{(a_f + a_{f8}) \cdot 0.5 + a_{f1} + a_{f2} \dots + a_{f7}}{8} \quad (1)$$

$$a_o = \text{Machined notch}(l) + \text{Original crack}(l) \quad (2)$$

The fatigue crack length (mm) measurements were taken at 9 equidistant points located at 1% of the test plate thickness from the test plate surface, from point  $a_{f0}$  to  $a_{f8}$  as shown in Figure 2. The calculation of the fracture tests for 0.2 % proof strength according to the temperature was derived from BS 7448 Part 2:1997, as shown in Equation (3),<sup>[11]</sup> where T is the experimental temperature;  $\sigma_{Y0}$  is fatigue crack temperature ; and  $\sigma_Y$  is fracture test temperature.

$$\sigma_Y = \sigma_{Y0}(\text{room temp}) + \frac{10^5}{(491 + 1.8 \cdot T)} - 189 \quad (3)$$

For the CTOD test, a three-point bending tester (IMN universal machine) was utilized to measure

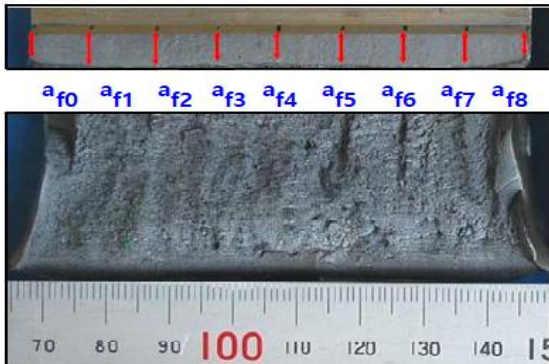


Fig. 2 Location of measuring point for specimen

the force and opening displacement at 10 Hz with a voltage and strain meter. The measurement was taken 2 mm below the crack on both sides because the test plate was immersed in a dry ice mixture for 40 minutes to maintain a temperature of  $-10 \pm 2^\circ\text{C}$ , and the temperature retention time was set to 30 s/mm. BS 7448 : Part 1 : 1991, and the bend specimens calculation formula ( $K_Q$ ) is expressed in Equation (4).<sup>[10]</sup> The calculation of the stress intensity factor ( $K_C$ ) is shown in Equation (5)<sup>[10]</sup> with the maximum force  $P_{\max}$  and correction coefficient ( $Y(\lambda)$ ), where the correction coefficient is defined as the actual crack length divided by the width of the specimen,  $S_{pan}$

$$K_Q = \frac{F_Q S}{B W^{1.5}} \cdot f\left[\frac{a_0}{W}\right] \quad (4)$$

$$K_C = \frac{P_{\max} \cdot S \cdot Y(\lambda)}{B \cdot W^{1.5}} \quad (5)$$

To define the load value in the event of unstable fracture, the stress intensity factor in Equation (5) is modified to be expressed as Equation (6)<sup>[10]</sup> to be substituted for the actual measured value.

$$(Y_\lambda) = \frac{3\lambda^{0.5} [1.99 - \lambda(1 - \lambda)(2.15 - 3.93\lambda + 2.7\lambda^2)]}{2[1 + 2\lambda][1 - \lambda]^{1.5}} \quad (6)$$

Based on the bend specimens calculation formula (4), the stress intensity factor ( $K_C$ ) and the correction coefficient ( $Y(\lambda)$ ) under an unstable fracture load, which is the formula given in BS 7448, Part 1: 1991, were derived, as shown in Equation (7), CTOD( $\delta_C$ ).<sup>[10]</sup>

$$\delta_C = \frac{K_C^2 \cdot (1 - \nu^2)}{2\sigma_Y E} + \frac{0.4(W - a_0) \cdot V_p}{0.4(W - a_0) + a_0 + Z} \quad (7)$$

Where E: Young's modulus 206 GPa,

$\nu$ : Poisson's ratio (0.3),

S: Span 4W,

B: width of test specimen,

$a_0$ : original crack length(mm),

$K_C$ : stress intensity factor (MPa),

$V_p$ : displacement,

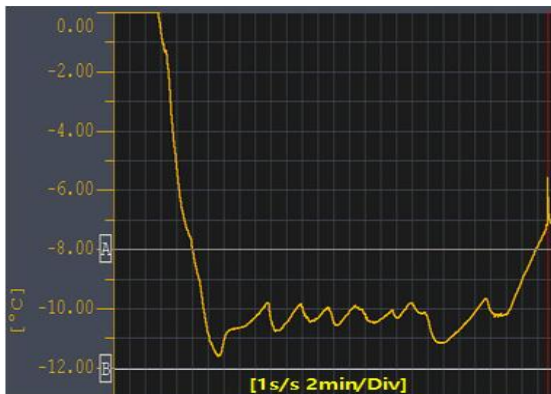
$V_g$ : permanent displacement of the notch at the crack end point replaced by permanent deformation displacement

and Z: thickness between the clip gauge and the end of the specimen.

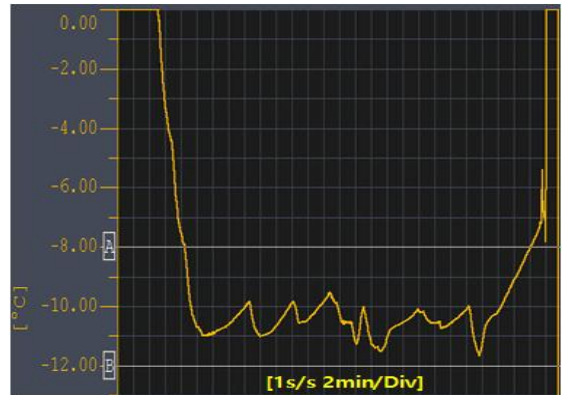
### 3. Experimental results and discussion

#### 3.1 Fatigue pre-cracking length and original crack length(FCAW)

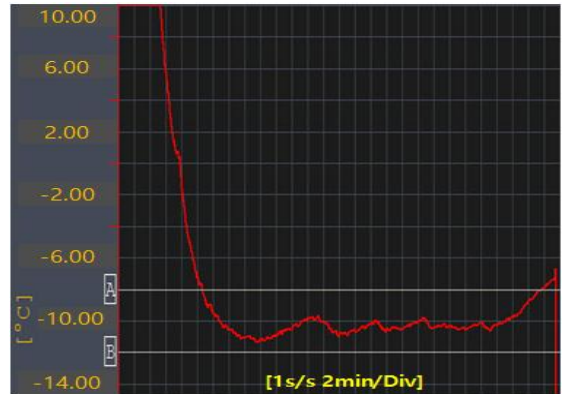
In this experiment, the fatigue pre-crack measurement test was conducted to detect the presence of the tunneling effect on a specimen over 80 mm when the fatigue crack exists by using the three-point bending tester in accordance with BS 7448. The crack point continued until both surface cracks reached the target length, and Fig. 3 indicated a change in the FCAW specimen temperature distribution of three specimens (a, b, c).



(a)



(b)



(c)

Fig. 3 Temperature distribution change for FCAW

Table 4 Results for 9 crack length of the fatigue crack

Specimen	No	Spec #1	Spec #2	Spec #3
Original crack length (mm)	$a_1$	37.4	38.5	38.8
	$a_2$	39.0	39.7	39.6
	$a_3$	39.1	39.3	39.1
	$a_4$	38.8	39.2	38.6
	$a_5$	38.8	39.0	38.8
	$a_6$	38.9	39.0	38.9
	$a_7$	39.3	39.7	39.0
	$a_8$	39.6	40.0	49.2
	$a_9$	38.9	39.5	38.2
	$a_0$	39.0	39.4	39.0
Difference of each crack	$a_0/W$	0.507	0.512	0.507
		0.055	0.037	0.035

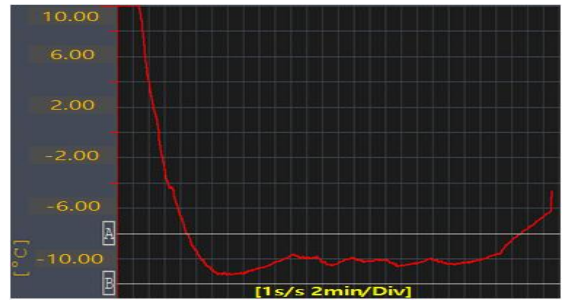
**Table 5 Results for fatigue pre-cracking parameters**

Specimen No	Spec #1	Spec #2	Spec #3
Maximum fatigue pre-cracking force( $F_f$ )	75 kN		
Stress ratio( $R$ )	0.1		
Maximum fatigue stress intensity factor ( $K_f$ )	38	39	38
Cyclic No (Cycles)	32692	28959	26818
$\Delta K/E(m^{1/2})$	0.0001670	0.0001700	0.000167
Stress intensity factor( $K$ )	145	151	151

The Y coordinates indicate temperature, and the X coordinates indicate time. For 80mm thick steel with a scale of 0.5 minutes per scale, the set temperature of  $-10^{\circ}\text{C}$  was maintained for 40 minutes to satisfy the rule's requirements. This indicates that the BCA steel has secured the product's reliability in temperature control at FCAW maximum heat input of 34.4 kJ/cm. Table 4 and 5 display the FCAW's initial crack length measurements and the fatigue pre-cracking results, respectively.

The applied load at the final stage of fatigue crack expansion was set to 75 kN, so as to reduce damage to the properties of the specimens; the frequency was set to 10 Hz and the stress ratio to 10:1. The maximum fatigue stress intensity factors applied in the fatigue crack stress phase were similar for all three specimens; while specimen 1 had more than 32,000 cycles, the other two specimens had ratios of less than 30,000 cycles. The results are detailed in Table 5.

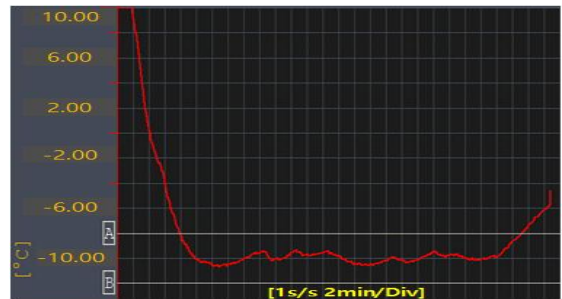
In addition, the stress intensity factor, which is the most important parameter in fracture mechanics, is an average 149MPa for the three specimens. The crack length may be observed to be directly proportional to the value of the stress intensity factor, and it increases the severity or risk of stress near the crack.



(a)



(b)



(c)

**Fig. 4 Temperature distribution change for FCAW**

### 3.2 Fatigue pre-cracking length and original crack length(SAW)

SAW can reduce welding time by more than three times than that of FCAW techniques, but the grains of welds may increase due to the high heat input, resulting in a reduction in toughness. There is an active study on the effect of grains<sup>[7-9]</sup> on the weld toughness, but the SAW test was conducted in the same way as FCAW because it was necessary

to verify the effect of the heat input of the thick or extra thick plate on weld grains. Figure 4 illustrates the changes in temperature distribution of the three specimens produced by the SAW method.

All three specimens are maintained between A (-8°C) and B (-12°C) for an average of 40 minutes at the set temperature of -10°C; this may be interpreted as maintaining product reliability in terms of temperature control even when applying SAW, a high heat input welding process. Table 6 and 7 present the initial crack length of the fatigue crack by SAW and the result of fatigue pre-cracking parameters.

**Table 6 Results for 9 crack length of the fatigue crack**

Specimen	No	Spec #1	Spec #2	Spec #3	
	$a_1$	38.2	38.7	37.9	
	$a_2$	40.0	40.0	39.6	
	$a_3$	39.9	39.0	39.5	
	$a_4$	39.6	39.1	39.3	
Original crack length (mm)	$a_5$	39.1	39.3	38.7	
	$a_6$	38.7	39.7	38.5	
	$a_7$	38.7	39.9	38.6	
	$a_8$	39.2	40.1	39.3	
	$a_9$	38.9	38.5	38.4	
	$a_0$	39.2	39.5	38.9	
	$a_0/W$	0.510	0.514	0.507	
	Difference of each crack		0.047	0.040	0.044

**Table 7 Results for fatigue pre-cracking parameters**

Specimen No	Spec #1	Spec #2	Spec #3
Maximum fatigue pre-cracking force( $F_f$ )		75 kN	
Stress ratio( $R$ )		0.1	
Maximum fatigue stress intensity factor ( $K_f$ )	39	39	38
Cyclic No (Cycles)	30680	32065	29780
$\Delta K/E(m^{1/2})$	0.000170	0.000171	0.000168
Stress intensity factor( $K$ )	153	146	144

The maximum fatigue stress intensity factors in the fatigue crack stress stage are similar for each specimen. The ratio of the strength factor to the elasticity coefficient was calculated at an average of 30000 cycles, and the three-specimen average stress intensity factor is 147.6 MPa  $m^{1/2}$

### 3.3 Crack tip opening displacement test for FCAW and SAW

The CTOD test is generally applied to the characteristic evaluation of the resistance to the forward crack of welds, and the pattern of variation is also significant depending on the test temperature. For temperature-dependent fragility changes, the material is brittle destroyed in the range between high and low temperatures, but plastic deformation behavior is also seen in load and displacement curves during the test. Therefore, a three-point bending CTOD test was conducted to evaluate the specimens' fracture toughness by substituting the bending specimen formula (4) according to BS 7448: Part 1: 1991. For this method, the bending load is applied to the entire specimen through the bending operation after rapid cooling of the specimen and causes local plastic deformation at the notch end. In addition, the procedure is simple, and the size of the load on the specimen is small because it causes plastic deformation of the material from the notch root. The coefficient of reverse bending stress is obtained by generating a constant tensile residual stress and substituting the maximum value of the bent load; a value that is obtained using the cycle for Equation (8). Here,  $L$  is a typical square-shaped specimen notch constraint, and  $w_{rb}$  represents the size of the plastic region resulting from the reverse bending.

$$K_{rb} = LR_{p0.2} \sqrt{\frac{8w_{rb}}{\pi}} \quad (8)$$

Fig. 5 and 6 show how each of the three specimens were prepared and analyzed through the processes of FACW and SAW, respectively.



(a)



(b)



(c)

Fig. 5 Fracture surface specimen of FCAW



(a)



(b)



(c)

Fig. 6 Fracture surface specimen of SAW

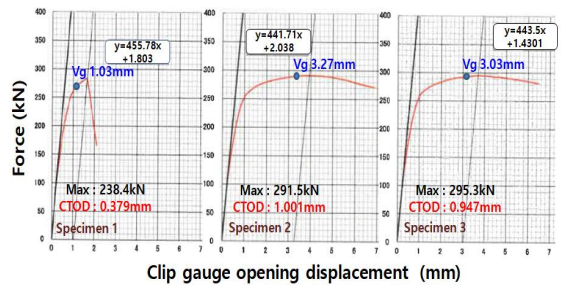


Fig. 7 Results of force and crack opening displacement for FCAW

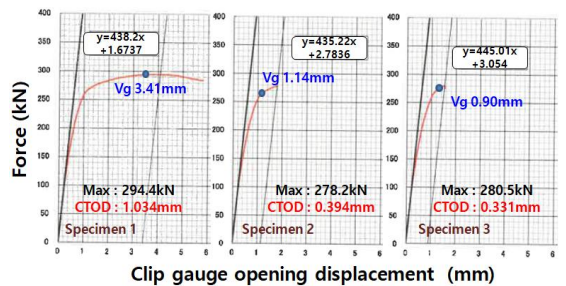


Fig. 8 Results of force and crack opening displacement for SAW

**Table 8 Results for CTOD value**

Weld type	$(V_p = V_g)$ ( mm)	Max force (kN)	CTOD (mm)
FCAW	2.44	290.06	<b>0.775</b>
SAW	1.81	284.36	<b>0.586</b>

Experiments were conducted after forming fatigue cracks at regular intervals on the notches of test pieces manufactured by two different processes. The load ( $P$ ) from the load cell and the displacement ( $V_p = V_g$ ) from the clip gauge attached to the notch were identified. Figures 7 and 8 show the displacement measurements for each specimen under load. In the case of specimen 1, which was manufactured by the FCAW method, a pop-in phenomenon occurred. This phenomenon is a sudden load displacement that occurs shortly after the material's anti-welfare point in Figure 7. As the load increases, unstable fractures can cause such destruction in areas where the objects were aggregated at the end of the crack or areas that are partially vulnerable due to uneven materiality. In this case, the load ( $\delta_C$ ) when the destruction reoccurs is defined by Equation (7).

For the other two specimens, there was no unstable fracture during the test, and the crack progressed stably. As the load and displacement increased, the displacement ( $V_g$ ) at the notch from the 3 mm point and with a maximum load of CTOD were 1.001 mm and 0.947 mm. This was significantly above the acceptable CTOD values, as recommended by the American Petroleum Institute.

Figure 8 shows the results of the SAW process as applied to the three specimens. To obtain the total displacement results, a line parallel to the elastic load slope is drawn, and the CTOD result is derived from the maximum load and the displacement of the notch part. Except for specimen 1, the maximum displacement interval length is 1.14 mm. Small substances from the weld pool and slug

generation during automatic welding have been accumulated at the crack end. Such fractures are interpreted as a localized destruction phenomenon in the section before the initial crack. The application of SAW welding processes with high heat input to BCA steel has been found to be resistant to longitudinal strength vulnerabilities in container ships. In addition, the thickness of the steel, weld quality management, and welders' skills are also key variables. Table 8 presents the average CTOD experimental results of the FCAW and SAW specimens of EH40 BCA-TMCP (80t) steel.

## 4. Conclusions

To secure longitudinal strength, the lack of which is a disadvantage of container ships, the following conclusions can be obtained through the two different welding process (FCAW and SAW) with CTOD test depending on the stress intensity factor at the crack end with high heat input:

1. In an experiment on the length of fatigue pre-crack, the stress intensity factor proportional to the length of the crack was similar regardless of the heat input.
2. In the macroscopic deformation behavior of the test specimen, it was found that the displacement in the notch of FCAW was 26% less likely to occur in plastic deformation than in SAW.
3. CTOD shows that FCAW, which has lower heat input, maintains more of the specimens' properties than SAW.
4. Currently, welding parts of high-intensity, high-strength steel with a thickness of above 80mm are mainly welded by FCAW (manual) to ensure safety. However, it is costly and takes about four days to complete. On the other hand, welding with SAW (automatic) takes 1 to 2 days. This study provided the basis for how the application of the SAW process affects the weld integrity of extra thick plates.



## Acknowledgements

This paper was supported by Research Grant of Dong-A University

## REFERENCES

1. Handa, T., Suzuki, S., Tokura, M., Kiji, N., Nakanishi, Y., "Behavior of long brittle crack arrest in Tee joint structure of thick plate," Bulletin of the Japan Society of Naval Architects and Ocean Engineering, Vol. 4, pp. 461-462, 2007.
2. Honda, T., Kubo, T., Kawabata, F., Nishimura, K., Suzuki, S., Shiomi, H., Miyata, T., "Effect of Kca value on behavior of brittle crack arrest in Tee joint structure of thick plate," Bulletin of the Japan Society of Naval Architects and Ocean Engineering, Vol. 4, pp. 459-460, 2007.
3. Inoue, T., Ishikawa, T., Imai, S., Koseki, T., Hirota, K., Tada, M., Kitada, H., Yamaguchi, Y., Yajima, H., "Long crack arrestability of heavy thick shipbuilding steels," Proceedings of the 16<sup>th</sup> International Offshore and Polar Engineering Conference 2006.
4. International Association of Classification Society, Application of YP47 steel plates, UR W31 rev.1 (2015)
5. An, Y. H., Bae, H. Y., Song, W. H., Jeong, B. Y., Hwang, W. T., Noh, H. D., "Welding Solutions for Brittle Crack Arrest in EGW Welded Joints of Ultra Large Container Ships," Collection of Special Lectures and Academic Presentation by the Korean Welding Society, pp. 140-140, 2019.
6. Choi, K. S., Lee, S. H., Chung, W. J., Hwang, H. G., Hong, S. H., Hong, J. H., "Study of Brittle Crack Propagation Welding for EH40 Steel Plate in Shipbuilding Steel," Journal of Korean Society of Manufacturing Process Engineers, Vol. 18, No. 5, pp. 9-16, 2019.
7. Smith, N. J., Mcgrath, J. T., Gianetto and R. F. Orr., "Microstructure/Mechanical/Property Relationship of Submerged Arc Welds in HSLA 80 Steel, Welding Journal," 68-3, pp. 112-120, 1989.
8. Mcgrath, J. T., Gianetto, J. A., "Some Factors Affecting the Notch Toughness Properties of High Strength HY80 Weldments, Canadian Metallurgical Quarterly," 25-4, pp. 349-356, 1987.
9. Glover, A. G., Mcgrath, J. T., Tinkler, M. J., Weatherly, G. C., "The Influence of Cooling Rate and Composition on Weld Metal Microstructures in a C/Mn and HSLA Steel, Welding Journal," 56-9, pp. 267-273, 1977.
10. BS7448: Part 1 : 1991, "Fracture Mechanics Toughness Tests, Part 1. Method for the Determination of  $K_{IC}$ , Critical CTOD and Critical J Values of Metallic Materials," (British Standard)
11. BS7448: Part 2 : 1997, "Fracture Mechanics Toughness Tests, Part 2. Method for the Determination of  $K_{IC}$ , Critical CTOD and Critical J Values of Welding in Metallic Materials," (British Standard)